Optimisation of FE parameters used in fine numerical modelling of steel T-stub elements

Daniel L. Nunes[1,*], *Adrian* Ciutina[1], *Ioan* Marginean[2], *Florea* Dinu[2] and *Ivana* Tadić[2]

[1] Department of Overland Communication Ways, Foundation and Cadastral Survey, Politehnica University Timisoara, Romania

[2]Department of Steel Structures and Structural Mechanics, Politehnica University Timisoara, Romania

Abstract. In steel frame buildings the role of the beam-to-column connection is crucial for assuring structural integrity, and due to their complexity and non-linear behaviour, the bolted configurations of this type of connection are usually the most vulnerable elements of a building. In order to assess the behaviour of a bolted steel connection, the simplified model of the equivalent T-stub is used. Based on previous experimental studies on a parametric set of T-stubs, the aim of this study is to optimise a numerical model in order to validate the experimental data and produce a fully calibrated finite element model, created with Abaqus/Explicit FE software package. To model properly the nonlinear behaviour of the component, an analysis of the properties of the model was conducted regarding the finite elements properties, analysis properties and discretization. The solid finite element properties considered were such as the number of nodes, integration, contact and true stress-strain material definition, including damage criteria. In this context, the assembly was subjected to a transient quasi-static explicit FE analysis using mass-scaling features. The results are expressed by comparison of Force-displacement curves obtain via numerical analysis and experimental testing.

1 INTRODUCTION

The connections in steel frame structure play the most important role in providing enough ductility and capacity of the structure to resist progressive collapse caused by accidental loading such as impact, explosions, earthquakes etc. Being the most vulnerable elements within the structural system, the connections (Fig. 1) need to be able to support development of catenary forces in order to avoid progressive collapse [1]. Therefore, careful consideration must be paid to their design to ensure a suitable level of ductility and robustness as the avoidance of progressive collapse depends on the ability of the construction to transfer loads through alternative paths into adjacent members and finally to the foundations. In structures exploiting their full resistance, plastic hinges develop in the structural points where the forces exceed the plastic resistance of the member. In order to exploit the full plastic resistance, the structural members have to endure a certain plastic rotation without failure in selected points that could offer a ductile behaviour. In case steel moment resisting frames subjected to

* Corresponding author: daniel.nunes@student.upt.ro

extreme and destructive loading, the rotation and deformation capacity of the connection is of the primary importance to the development of alternative load paths through catenary action and is vital in enhancing the integrity for whole structure [2].

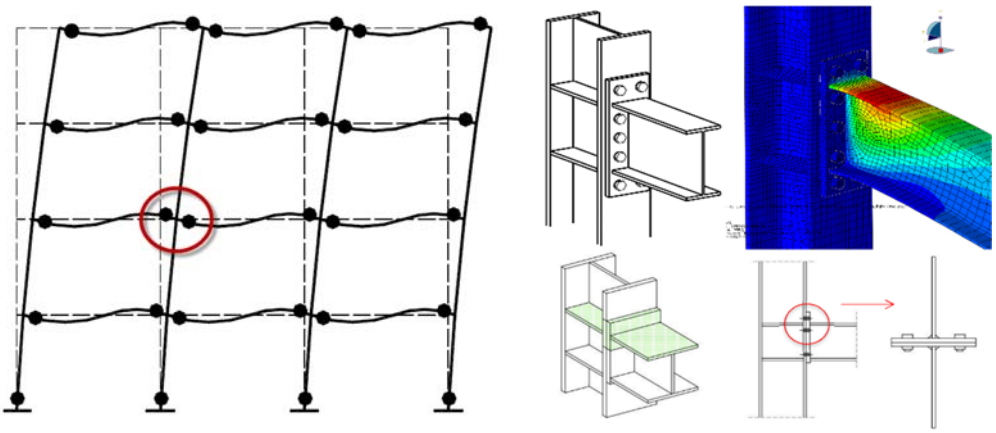

Fig. 1. Steel beam-to-column connections in moment-resisting frames

In order to attain the required characteristics of the connections special attention must be dedicated to designing all the components of joint. The most important component of bolted end plate beam to column connections is T-stub [3] asthis sub-system ensures the ductility of the connection and is used as the main indicator of its resistance. The behavior of such components depends on the material characteristics, bolt arrangement and geometry and it is accepted as a simplified model for the characterization of the behavior of the tension zone of a bolted joint.

2 EXPERIMENTAL PROGRAM

The main objectives of the experimental program were to investigate the capacity of bolted T-stub connections under large tensile deformations according to Eurocode demands and to predict the response of T-stub components [4]. The general configuration and dimensions of T-stub are shown in the Fig. 2 and their specific geometry is shown in Table 1.

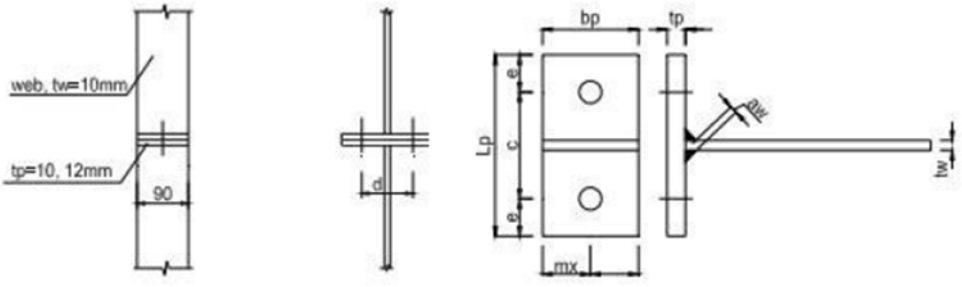

Fig. 2. T-stub geometrical configuration

The length of the web is 686 mm with thickness of 10 mm. The width of the web and flange is 90 mm with varying thicknesses of the end plate and the distance from the bolt

center to the edge of end plate is 30 mm on both sides. The T-stubs are designed to achieve ductile failure modes based on static loading conditions according to Eurocode 1993-1-8 [3].

Table 1. T-stub components tested configurations

	End plate thickness (mm)	Bolt diameter (mm)	Distance between the bolts (mm)
T-10-16-100	10	16	100
T-10-16-120	10	16	120
T-10-16-140	10	16	140
T-12-16-100	12	16	100
T-12-16-120	12	16	120
T-12-16-140	12	16	140
T-15-16-100	15	16	100
T-15-16-120	15	16	120
T-15-16-140	15	16	140
T-18-16-100	18	16	100
T-18-16-120	18	16	120
T-18-16-140	18	16	140

Table 2. Results for the material tests

Part	Thickness (mm)	Material	Yield strength (N/mm^2)
T-stub web	10	S355	390
T-stub flange	10	S235	310
T-stub flange	12	S235	305
T-stub flange	15	S235	275
T-stub flange	18	S235	420
Bolt	16	10.9	965

Prior to the T-stub tensile testing, individual tensile tests were carried for the material coupons representing each type of steel plate and bolt according to EN ISO 6892-1. The results are shown in Table 2.

3 NUMERICAL ASSESSMENT

In case of FE numerical analyses, two main types of numeric approaches are generally considered, Implicit and Explicit, which are often used for nonlinear dynamics:

- Explicit methods require a small-time increment size that is independent of the type and duration of loading. Simulations generally take on the order of 10,000 to 1,000,000 increments, but the computational cost per increment is relatively small.
- Implicit methods do not place a limitation on the time increment size. Implicit simulations typically take orders of magnitude fewer increments than explicit simulations.

However, since a global set of equations must be solved in each increment, the time cost per increment of an implicit method is far greater than that of an explicit method.

Although the Implicit method is considered as adequate for quasi-static and simple models, for more complex models it can give less accurate results than the Explicit method, which can also analyze problems involving complex contact interaction between many independent bodies.

3.1 Material property

The stress and strain relationship for a material represents the most used method to define how a material will react mechanically to an applied loading condition [5].

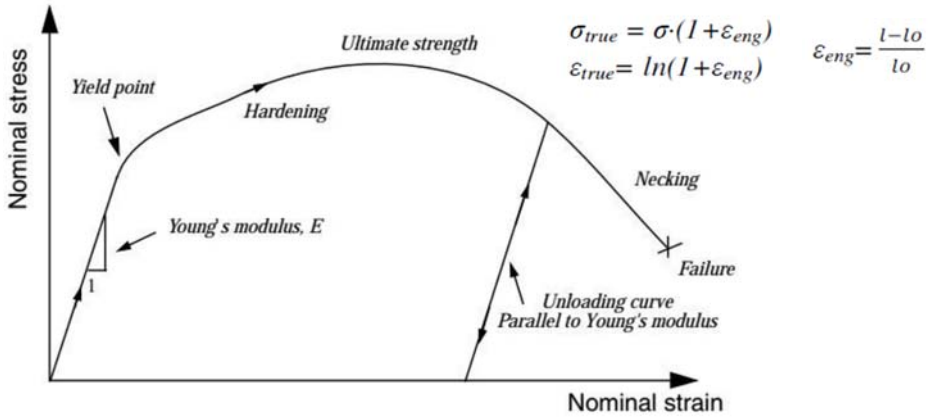

Fig. 3. Nominal stress/strain curve **[6]**

In order to define a linear-elastic steel material behaviour in Abaqus computer tool, two parameters were used, the Young's modulus of elasticity of 210 GPa and Poissons's ratio of 0.3. The value for density is 7.85x10-9 kN/mm^3. The material behaves elastically up to the yield point, after which starts the plastic deformation.

For the plastic material property modified stress-strain curves were used, different one for every coupon. These curves were obtained from standard tensile testing of steel coupons according to EN ISO 6892-1 [6]. Nominal stress-strain curves (Fig. 3) from experimental tests were then modified into true stress – strain curves according to equations given in Eurocodes EN-1993-1-5 Annex C6 [7].

Generally, the steel material deforming plastically under a tensile load may experience highly localized extension and thinning, already described as a necking zone, recorded during the failure of the specimen. These formulas are valid up to necking point, after which the steel material seems to soften while it actually hardens. Namely, during the plastic deformation of the steel material, its load bearing capacity per unit cross-section area increases, as a result of the strain hardening effect -Fig. 4. At the same time, the effective cross-section is reduced due to stretching of material.

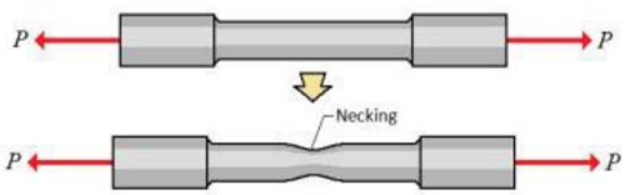

Fig. 4. Necking observed on a tensile test piece

As consequence, the stress/strain curve will run upwords as long as the strain hardening is increasing faster than the cross-section area is reducing. At some point the increase in strain-hardening will be overcome by the cross-section area reduction [5]. This practically represents the point of maximum load that the specimen can carry. Fig. 5 represents as example the nominal and true stress-strain curves for coupon P-20 with a thickness of 20mm.

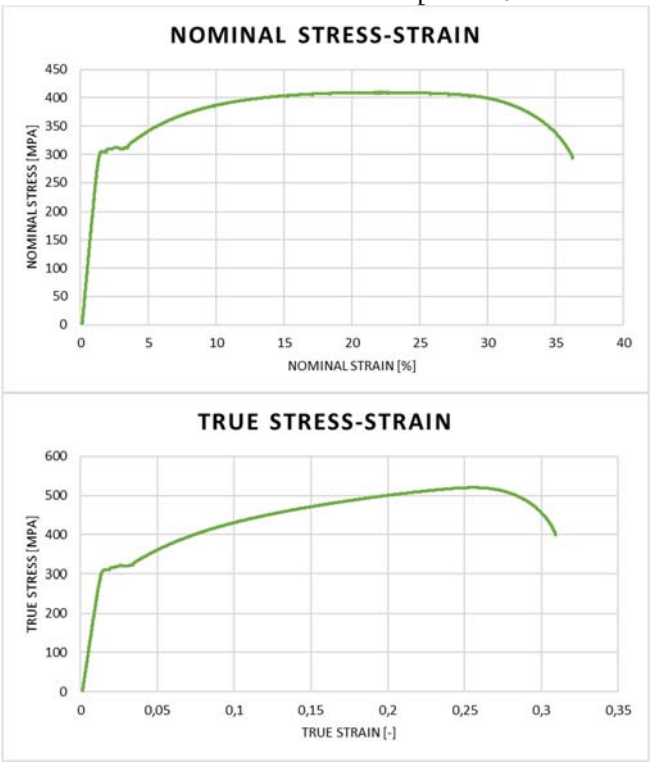

Fig. 5. Nominal and true stress-strain curves

3.2 Damage criteria

Damages in structures are caused by degradation of material due to initiation and growth of micro cracks in a real-life material element. Due to micro-granular irregularities, some zone in the original material form irregularities under the form of weak zones, that will not be able to carry the loading applied. The loading will cause a weaker area to strain further than the rest of the model, even if the load is not increased.

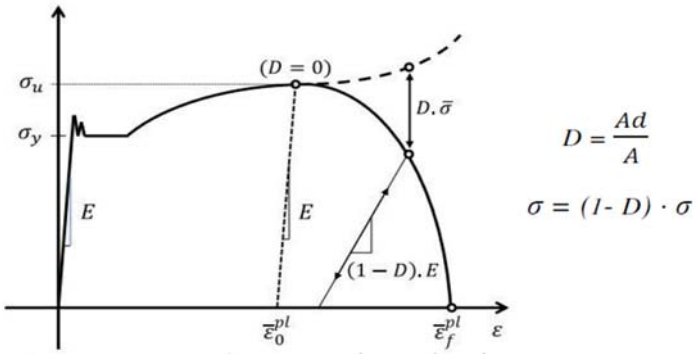

Fig. 6. Material curve with progressive damage degradation **[10]**

In Abaqus computer FE tool the final fracture is characterized using the Damage Initiation criterion and Damage Evolution for ductile materials through different coefficients. This material property defines the behaviour of material after reaching the ultimate strength i (Fig. 6). The input data to the fracture model was obtained by running the model without this fracture criterion. Further, the average value of the equivalent plastic strain for the elements that were supposed as failed, was measured at the point of the final fracture. This strain value is actually used as the damage initiation criterion. It is important to note that the values of the coefficients depend on the mesh size and shape as mentioned in [8]. Damage evolution option is defined using tabular softening type. The coefficients used in case of T-stub analyses are shown in Table 3.

Table 3. Coefficients used in the Ductile Damage criteria

Coupons	Fracture strain	Stress Triaxiality	Strain Rate	Ductile damage-Type displacement	
				Tabular softening	
P19	0.35	0.8	0.5	0	0
P20	0.61	0.8	0.5	0.25	0.4
P21	0.55	0.8	0.5	1	0.8
P22	0.65	0.8	0.5		
P23	0.37	0.8	0.5		

3.3 Discretization

The influence of different mesh size of elements can be described in function of dissipation of energy. With mesh refinement dissipated energy decreases. The dissipated energy is treated as an additional material parameter, and it is used to compute the displacement at which full material damage occurs. Up to the point of ultimate strength the plastic properties are the same for different mesh size, but at higher strain values, the plastic behaviour is dependent on the element size. Since the post-critical behaviour is dependent on the mesh size, the engineering stress/strain curve cannot be directly used to mechanically model the material: in a FE model the continued elongation of the model is concentrated into straining of a few elements. For this deformation the element size is crucial. Since the elongation is produced through even one single element, the properties of this element will govern the behaviour of the whole model [5]. Therefore, the global response for the coarser mesh will be stiffer than for the finer mesh.

In order to enhance the fine response in case of T-stub models, linear hexahedral elements were used for meshing (8-node brick C3D8R) with reduced integration and enhanced hourglass control.

3.4 Material calibration results

The experimental force/displacement behaviour was validated numerically and different material properties and mesh sizes were set to be further used in T-Stub models.

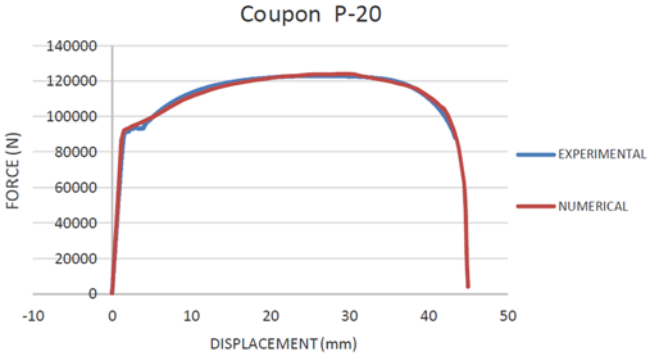

Fig. 7. Numerical and experimental comparison (for coupon P20)

Fig. 7 shows the numerical response curve with respect to the traction test on coupon, based on the force-displacement curves. The results show a very good approximation of the model behaviour of the coupons, showing insignificant errors smaller than 2% to testing.

3.5 T-stub numerical analysis

In order to validate experimental data and the obtained results, a numerical model is generated with Abaqus/Explicit FE package. The models are created using precise measurements evaluated before testing of the specimens. Material properties are determined using experimental coupons tests previously mentioned. The nominal diameter of the bolt is 16mm. However, its real diameter is less than 16 mm due to the thread: thus, the actual diameter was evaluated according to standard ISO 898-1:2009 [9].

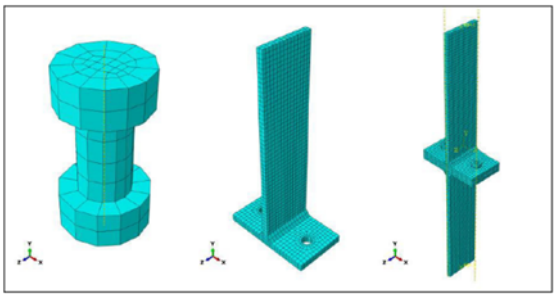

Fig. 8. T-stub elements discretization

In order to carry out the parametric study, numerical models were validated against experimental ones and then calibrated by increasing the distance between the bolts. The validation was done using F-δ response which offers the overall behaviour of T-stub elements. The models used for validation were specimens T-10-16-100, T-10-16-140, T-15-16-100 and T-15-16-140.

4 NUMERICAL RESULTS

Fig. 9 and Fig. 10 show the validation of T-stub models through numerical and experimental force-displacement curves . The numerical results were compared with the experimental data through force-displacement response and showed good correlation.

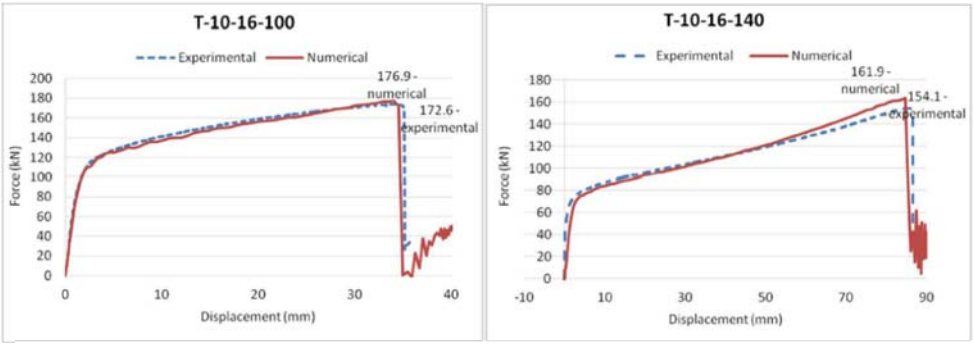

Fig. 9. Comparison between numerical and experimental results – T-10

The numerical models accurately predict the actual behaviour of the T-stub specimens, proving a good accuracy for the elastic stiffness and the plastic transitions. Differences in yield force, ultimate displacement and initial stiffness are less than 10% error range.

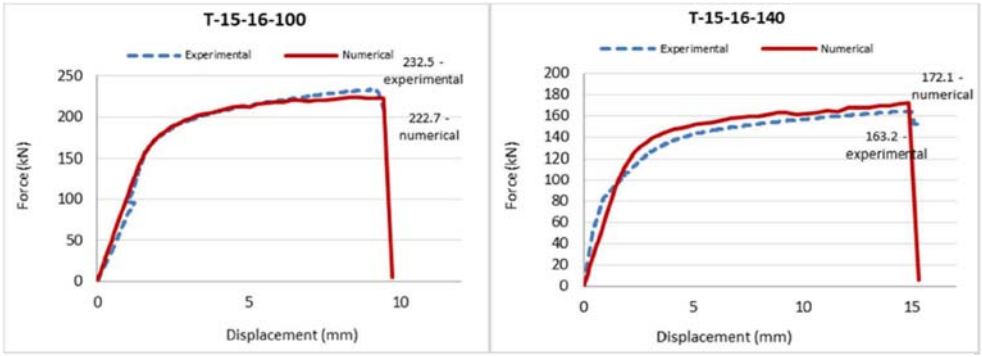

Fig. 10. Comparison between numerical and experimental results – T-15

Fig. 11 shows the deformed shape of the T-10-16-140 model under the form of equivalent plastic strain map in comparison with the corresponding deformed specimen after experimental testing. The FE model follows with high accuracy the actual behaviour of the tested specimen and shows similar failure mode.

The generally accuracy of the results between the experimental tests and the numerical models show the validity of the calibration method with high accuracy, can be further considered to more complex configurations. The presented example shows that if enough experimental information is collected at the basic level of the material properties, increasingly complex models can be developed, allowing for the development of more accurate technical solutions for problems with high dependency of the accuracy of the initial conditions, such as cyclic loading of connections.

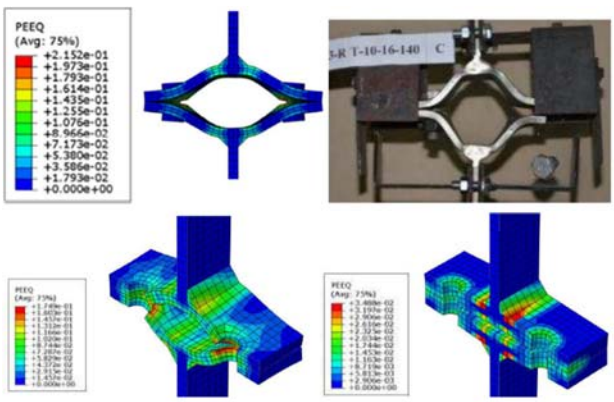

Fig. 11. Deformed shapes before failure

5 CONCLUSIONS

The paper presents the way in accurate FE modelling. The study leads to the following main conclusions:

- a satisfactory match can be obtained between experimental and numerical results provided that a thorough calibration phase is conducted;
- the calibration of the material behaviour is especially important: it should follow the European standards recommendations for true stress-strain characterization and damage criteria should be added and calibrated based on parameters such as fracture strain, stress triaxiality and strain rate;
- the size of the mesh is equally important and it should suffer minimal changes after the calibration process;
- the significant variability of the characteristics of the delivered steel is an important factor and can significantly affect the reliability of numerical results. Therefore, material tensile testing needs to be carried out in order to provide a good basis for the calibration process.

6 ACKNOWLEDGEMENT

This work was supported by a grant of the Romanian National Authority for Scientific Research and Innovation, CNCS/CCCDI - UEFISCDI, project number PN-III-P2-2.1-PED-2016-0962, within PNCDI III: “Experimental validation of the response of a full-scale frame building subjected to blast load” - FRAMEBLAST (2017-2018).

7 BIBLIOGRAPHY

[1] F. Dinu, I. Marginean and D. Dubina, “Experimental testing and numerical modelling of steel moment-frame connections under column loss,” *Engineering Structures,* no. 151, 2017.

[2] F. Dinu, “Structural conception and collapse control performance based design of multistory structures under accidental actions,” Timisoara, Romania, 2012-2016.

[3] CEN, EN1993-1-8 Eurocode 3: Design of steel structures - Part 1-8 Design of joints, 2005.

[4] F. Dinu, D. Dubina, I. Marginean, C. Neagu and I. Petran, "Axial strength and deformation demands for T-stubs connection components at catenary stage in the beams," in *8th International Conference on Behavior of Steel Structures in Seismic Areas*, Shanghai, 2015.

[5] H. Levanger, Simulating Ductile Fracture in Steel using the Finite Element Method: Comparison of Two Models For Describing Local Instability due to Ductile Fracture, Oslo: Faculty of Mathematics and Natural Sciences, University of Oslo, 2012.

[6] CEN, "Metallic materials - Tensile testing - Part 1: Method of test at room temperature," 2016.

[7] CEN, EN1993-1-5 Eurocode 3: Design of steel structures - Part 1-5 Plated structural elements, 2006.

[8] G. A. Anwar, Ultimate deformation and resistance capacity of bolted T-stub connections under different loading conditions, Timisoara: Politehnica University of Timisoara, 2017.

[9] Internation Organization for Standardization, ISO 898-1: Mechanical properties of fasteners made of carbon and alloy steel - Part 1: Bolts, screws and studs with specified property classes - Coarse thread and fine pitch thread, ISO, 2009.

[10] Dassault Systèmes, *Abaqus FEA 14.1,* https://www.3ds.com/products-services/simulia/products/abaqus/, 2016.